

## Study on Sound Absorption of Road Acoustic Screens Under Simulated Weathering

Artur NOWOŚWIAT, Jerzy BOCHEN, Leszek DULAK, Rafał ŻUCHOWSKI

*Faculty of Civil Engineering  
Silesian University of Technology  
Akademicka 5, 44-100 Gliwice, Poland;  
e-mail: {artur.nowoswiat, jerzy.bochen, leszek.dulak, rafal.zuchowski}@polsl.pl*

*(received April 11, 2017; accepted January 5, 2018)*

The present paper is comparing the results of research studies carried out for three road acoustic screens of different design and different number of damping layers. For the tests, we selected timber or steel screens with a traditional multilayer structure and also one innovative type of simplified design. With respect to particular panels, their sound absorption properties were investigated in the reverberation chamber after they had been subjected to simulated weathering. In the process, two screens were subjected to the aging tests of 50–500 cycles in a special climatic chamber, and the innovative screens were subjected to 1000 cycles. The procedure was repeated every 50 or 100 cycles in order to obtain the changes of acoustic characteristics. The changes taking place in the absorbing material were also investigated with the use of scanning electron microscopy method (SEM). Basing on the obtained results and on the statistical analysis, the capability to maintain acoustic properties by the panels during their service life in natural conditions was estimated. For that purpose, linear statistical models were worked out, which were then applied to estimate the value of the single number sound absorption coefficient after successive aging cycles as well as the predicted time periods of acoustic class changes.

**Keywords:** acoustic screens; ageing process; sound absorption; durability.

### 1. Introduction

In the extremely urbanized environment that we are witnessing worldwide, communication is becoming more and more important. The research studies involving vibration and noise around roads have been focused on the influence of vibration on bridges and their resistance, as well as on the reduction of noise in the environment (MEAKAWA, 1968; KURZE, ANDERSON, 1971; FUJIWARA *et al.*, 1977).

Acoustic screens are commonly applied to reduce the level of noise in the vicinity of roads. A lot of research studies have been focused on the shape of such screens (MAY, OSMAN, 1980; MURATA *et al.*, 2006) or on sound absorbing materials used in them (FUJIWARA *et al.*, 1998; ISHIZUKA, FUJIWARA, 2004).

Acoustic panels applied in road screens must satisfy specific requirements involving sound absorption quality. Such requirements are usually verified in laboratory conditions, without long-term exposition to atmospheric factors. In order to find out in what way

the exposition in the natural environment may influence acoustic properties, additional climatic tests were carried out in simulated conditions. As a rule, the tests on road acoustic screens usually involve the aspect of sound absorption, sound insulation and intrinsic sound diffraction of the added devices as their main function (GARAI, GUIDORZI, 2008; GUIDORZI, GARAI, 2013). And therefore, many problems pertaining to their main function have been tested, i.e. the structure and design of screens, including among others cross-section types of noise screens (WATTS, MORGAN, 1996), types of applied materials (SAMUELS, ANCICH, 2001) or the phenomenon of diffraction in sound baffles (FUJIWARA *et al.*, 1977; LI, WONG, 2005; MIN, QIU, 2009). A lot of field studies have been also concentrated on the influence of screen edge irregularity on the dispersion of sound, and in effect on the efficiency of the screen. Such analyses and research results were published for example in the works (JOANSSON, 1972; PIERCE, 1974; HADDEN, PIERCE, 1981; PARNELL *et al.*, 2017). The impact of screen shape on its efficiency was also pre-

sented in the work (MONAZZAM, LAM, 2005). In particular, a lot of studies have been devoted to compare the T-shaped screen with the standard, straight one.

The research on the acoustic properties of various fibrous sound absorption materials was carried out in the work (DELANEY, BAZLEY, 1970). Acoustic properties are usually tested in laboratory conditions, ignoring the impact exerted by weathering. There have been relatively few research studies on the changes of acoustic properties of screens during their service life. For example, the work (RUDNO-RUDZIŃSKA *et al.*, 2008) investigated the efficiency of the acoustic screen in field conditions, allowing for the impact of weathering, and the work (GARAI, GUIDORZI, 2000) demonstrated the influence of the quality of assembly works or the applied external fitting elements, i.e. seals, on the acoustic parameters of the screen. And in the work (KAMISIŃSKI *et al.*, 2015), the authors presented novel solutions of sound diffusing screens resistant to atmospheric conditions. The weathering effects which have influence on the efficiency of the screen were also investigated in the work (WATTS, 2000).

Interesting research results involving the impact of moisture content in the material on its acoustic properties were published by YILMAZER and OZDENIC (2005). The results of their studies confirm that the aging of sound absorbing materials applied in acoustic screens in natural conditions has influence on sound absorbing parameters of these screens.

The research studies involving the impact of aging are based principally on the analysis of material changes in the natural and artificial conditions. The most reliable research results have been yielded by long-term aging tests in natural conditions over several years. For example, we can mention the tests carried out on building materials such as ceramic materials (BUTTERVORTH, 1964), masonry coatings (MOTOHOSHI, NIREKI, 1984), doors or windows (BROLIN, 1984), sheets from PVC or from fiberglass reinforced polyurethane (UEMOTO, FLAUZINO, 1984), external wall tiling system (YIU *et al.*, 2007). Such tests usually take a lot of time. Therefore, thanks to laboratory conditions offered nowadays, short-term tests are more frequently applied (LITHERLAND *et al.*,

1981; MOROPOULOU *et al.*, 2003; DING *et al.*, 2006; NOWOŚWIAT *et al.*, 2016), including for example atmospheric simulation chambers (MARTINEZ-RAMIREZ, 1997; PAVLIK *et al.*, 2004). Through the application of such chambers, we can test the resistance to different factors, e.g. moisture, low or high temperature, light or UV radiation. During the tests, we can determine physical or mechanical parameters (LITHERLAND *et al.*, 1981; KUS, CARLSSON, 2002; LANAS *et al.*, 2003). For acoustic screens, sound absorption is one of the vital parameters determining their efficiency. The basic assessment parameters are: the weighted sound absorption coefficient  $\alpha_w$  (ISO 11654, 1997) and the single number rating of sound absorption  $DL_\alpha$  (ISO 1793-1, 2012). The said quantities are used to determine the properties of absorption class, from the lowest A0 to the highest A5, depending on the value of the coefficient  $DL_\alpha$  (ISO 1793-1, 2012). The value of the weighted sound absorption coefficient is dependant principally on the parameters of the sound absorbing material. In most cases such acoustic assessment tests are carried out for the screens before their mounting. Some of such tests involve innovative acoustic screens (CASTIÑEIRA-IBAÑEZ, SÁNCHEZ-PÉREZ, 2015; MORANDI *et al.*, 2016).

Basing on the research experience of the authors (ŚLUSAREK *et al.*, 2014), we may say that under the influence of weathering, the values of sound absorption can undergo changes. In order to find out how the atmospheric factors can influence the acoustic properties of road acoustic screens, the tests on sound absorption were carried out for the selected types of panels of different design, which were subjected to weathering in simulated conditions.

## 2. Materials and research methods

### 2.1. Samples for tests

Three types of screens were prepared for the tests: timber design – variant T1 (Fig. 1a) and steel one, with one being of the combined structure – variant S2 (Fig. 1b) and the second innovative type of a simplified number of layers – variant S3 (Fig. 1c) de-

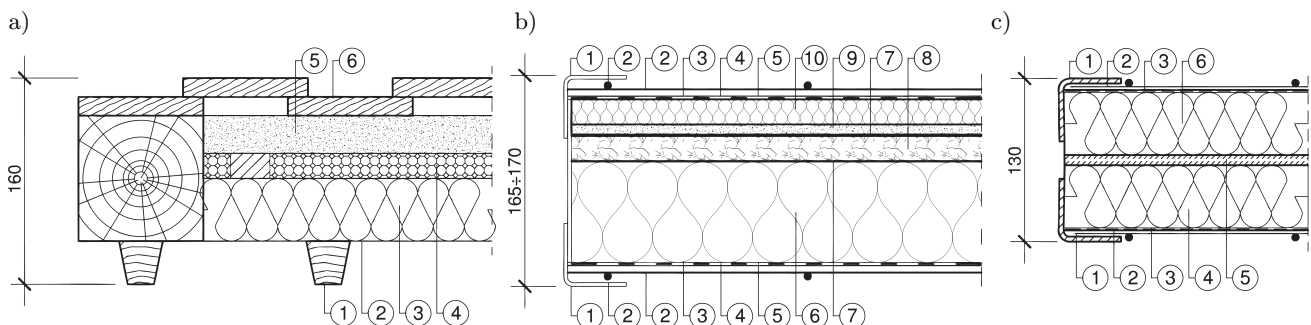


Fig. 1. The layered structures of tested acoustic panels: a) timber constructional T1 type, b) steel S2 type, c) steel S3 type.

scribed in the work (NOWOŚWIAT *et al.*, 2016). The dimensions of all panels were prepared as full-size samples accommodated to the size of the test fields of the climatic chamber so that the combined area had the required area of 10.0 m<sup>2</sup> according to (ISO 354, 2003). The panels of the timber frame (T1) had the dimensions of 0.95 × 1.50 m and the combined thickness of 160 mm. On one test wall of the aging chamber two samples were mounted (Fig. 2b). The arrangement of materials on the outdoor, absorbing side comprised: (1) diagonal wooden patches 35 × 35 mm spaced out every 15 cm, (2) protective grid from fiberglass, (3) mineral wool of the thickness 50 mm and density 80 kg/m<sup>3</sup>, (4) anti-erosion mat SECUMAT of the thickness 20 mm, black colour, (5) wood-chip concrete slab of the thickness of 20 mm, (6) two-layered perforated wooden board sheathing 15 × 120 mm from the back side, which makes altogether 5 layers (Fig. 1a).

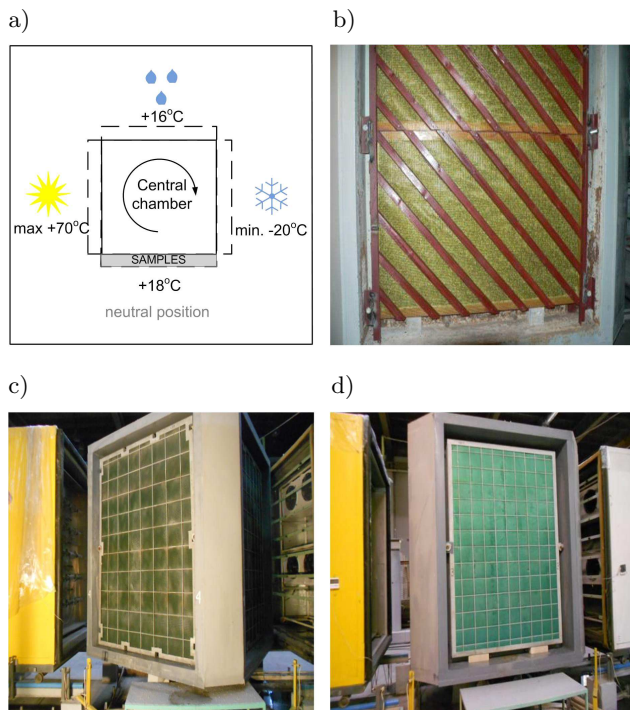


Fig. 2. a) Scheme of the simulated weathering chamber and views of the chamber with the sound screen samples: b) T1 samples, c) S2 samples, d) S3 samples.

The panels of steel design S2 were prepared with the dimension of 1.58 × 2.08 m and thickness 165 mm in a frame built from steel angle bars 50 × 50 × 4 mm (1) and from nets made from Ø8 steel ribbed bars galvanized every 15 cm (2), the same as the frame (Fig. 2c). The arrangement of the successive layers from external sides was as follows: (3) a protective grid PEHD, green colour, (4) a glass veil, black colour, (5) a double protective grid from glass fiber, yellow colour. Then from the absorbing side: (6) soft mineral wool of the thickness of 80 mm and density 100 kg/m<sup>3</sup>, (7) geotextile, white colour, (8) a struc-

tural mat 20 mm thick, black colour, (9) white geotextile, (10) a cement-bonded particleboard 8 mm thick, (11) hard mineral wool of the density of 120 kg/m<sup>3</sup> and thickness 20 mm, and then successively the layers as on the opposite side, altogether 12 layers (Fig. 1b).

The panels of steel S3 design are characterized by a standard arrangement of 5 layers with a special external fabric (3) (Fig. 1c). The fabric is made from thin glass fiber of the circular cross-section and diameter of the order of 5–10 μm forming woven flat banners (Fig. 9d). The panels measure 1.49 × 2.0 m and their combined thickness is 130 mm. The casing of the panels was made from the angles 50 × 50 × 3 mm (1) and grids on both sides made from steel ribbed rods Ø6 (2) spaced out at the distance of 150 × 150 mm galvanized like the angles. The inside of the panels was filled with mats from mineral wool of the thickness of 50 mm, separated with a cement-bonded particle board of the thickness of 10 mm (5) and shielded from the outside with the fabrics from glass fiber (3) of the green colour. From the absorbing side, we applied wool of the density of 80 kg/m<sup>3</sup> (4), and on the opposite side wool of the density of 120 kg/m<sup>3</sup> (6).

## 2.2. Simulated weathering test

For the simulation of atmospheric environment, a weathering rotational aging chamber was applied. The stand consists of four chambers (Fig. 2a) whereof the central rotational chamber is the main part which has four exposition walls of the dimensions 1.55 × 2.10 m for mounting the samples to be tested. The other three chambers cooperate with the central chamber and simulate the dominant weathering effects. The “sunshine” chamber provides the light radiation close to the natural solar radiation. The visible radiation within the wavelength of 400–700 nm is ensured by the system of 20 metalhalogene lamps of 8 kW generating the temperature of up to +70°C. An additional system of ultraviolet emitters of the wavelengths of 185 and 255 nm is emitting UV radiation. The “rain” chamber is imitating rain and wind. The amount of provided water and wind blowing is controlled in terms of amplitude, frequency and speed. Water is provided from the piping system and the minerals present in it are imitating rainwater containing impurities present in urban atmosphere. The “frost” chamber lowers the surface temperature of the investigated elements to –25°C.

One aging cycle comprises one rotation of the central chamber and lasts 4 × 50 min. The duration of the basic test of 100 cycles takes 4–5 weeks, depending on the number of cycles per 24 hours, which is usually 4–5 cycles. In order to ensure weathering similarity, the provided values correspond with mean multi-year average values. In the investigation studies, we accepted the climate of Upper Silesia region

in Poland as reference (50.310 N, 18.669 E). The activity of “frost” chamber was accepted as dominant due to the impact of  $0^{\circ}$  crossing temperature, which is line with the research studies of PIHLAJAVAARA (1984) and BASIŃSKA, KOCZYK (1995). Basing on the above, the average number of days with the freezing-thawing condition was taken into consideration, which for the averaged meteorological year is 41 days. Hence, 100 cycles correspond with the time period of 2.4 years in the natural conditions of the climate in Upper Silesia in Poland. Due to the increasing number of temperature values passing through  $0^{\circ}\text{C}$ , we accepted for the analysis that 100 cycles would correspond with the period of 2 years. The other relevant weathering parameters, as mean multi-year average, which were taken into consideration are as follows: the minimum temperature below zero  $-15.9^{\circ}\text{C}$ , the maximum sunshine temperature  $+59.5^{\circ}\text{C}$  for the accepted radiation absorption coefficient of 0.65, the intensity of sunshine radiation on vertical plane  $840\text{ W/m}^2$ , the volume of rainfall on horizontal plane on windy days 597 mm and the corresponding to it amount of diagonal rainfall on a vertical plane 335 mm for the average wind speed of 2.8 m/s (BOCHEN, 2010). The tests on the particular types of panels were carried out at different time periods and with different length of the tests: 150 cycles for T1 panels, 500 cycles for S2 panels and 450 cycles at the first stage for S3 panels (ŚLUSAREK *et al.*, 2014). Such a schedule was enforced by different requirements of the manufacturers. Nevertheless, due to uniform assessment criteria, the results are comparable. For the panels S3, due to minimum changes of acoustic parameters, a second stage of the studies was carried out, prolonging the simulated aging process with the additional 550 cycles (ŚLUSAREK *et al.*, 2015), during which distinctive changes of the acoustic properties were observed. The analysis of those research studies was presented in a separate paper (NOWOŚWIAT *et al.*, 2016).

### 2.3. Acoustic research studies of sound absorption

Sound absorption tests can be carried out by means of impedance tubes or in the reverberation chamber. Despite the fact that the investigation of sound absorption coefficient by means of impedance tube is easier, yet, due to technical and substantive reasons, the testing method in the reverberation chamber was selected. Such a choice was enforced first of all by the fact that the acoustic screen panels were subjected to research studies as a whole, together with the metal structure of the panels. Secondly, the class of acoustic screens was being defined in congruence with the Standard (ISO 11654, 1997), i.e. using the index  $DL_{\alpha}$ . Such an approach necessitates the application of reverberation chamber. The reverberation chamber used for the research studies was available at the Civil Engineering Department of the Silesian University of Technology in

Gliwice. The dimensions of that chamber are presented in Figs. 3a and 3b.

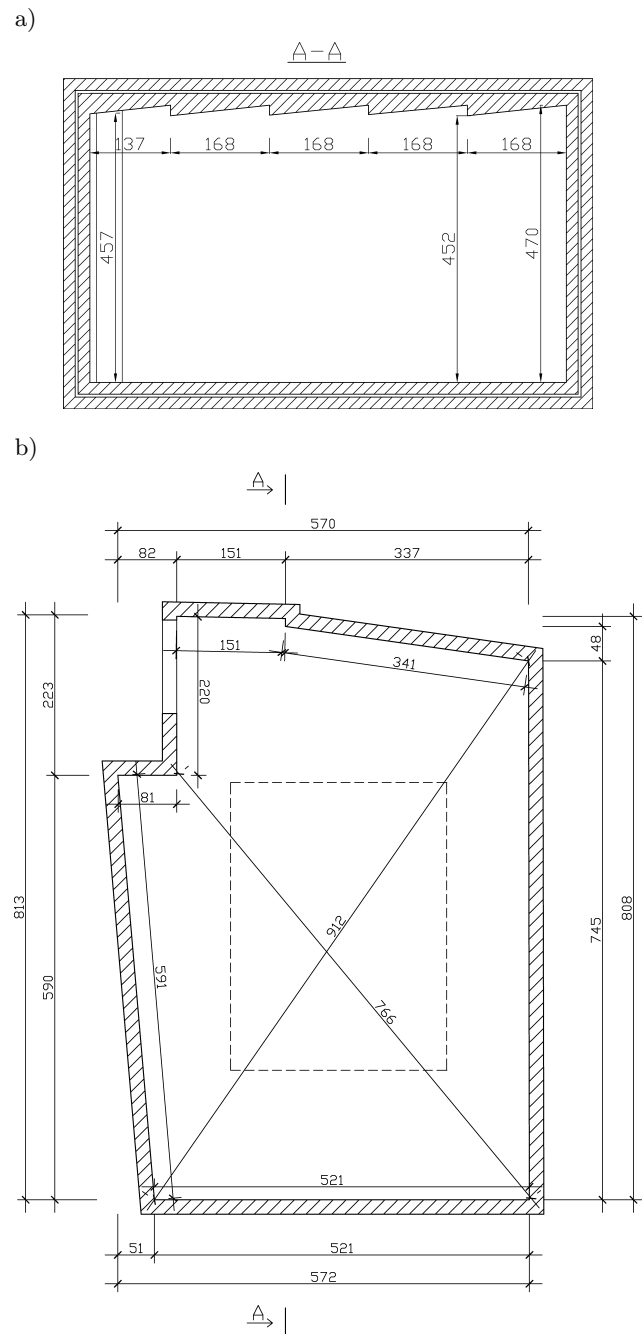


Fig. 3. Reverberation chamber: a) cross-section of the reverberation chamber, b) projection of the reverberation chamber.

The reverberation times for the empty reverberation chamber in which the studies were carried out, measured at constant temperature and relative humidity of air, the same as those applied for the measurement with material on the floor were respectively as follows:

100 Hz – 13.67 s, 125 Hz – 10.55 s, 160 Hz – 7.56 s,  
200 Hz – 8.66 s, 250 Hz – 9.43 s, 315 Hz – 8.02 s,

400 Hz – 6.85 s, 500 Hz – 6.43 s, 630 Hz – 6.06 s,  
800 Hz – 6.00 s, 1000 Hz – 5.70 s, 1250 Hz – 5.17 s,  
1600 Hz – 4.57 s, 2000 Hz – 3.86 s, 2500 Hz – 3.29 s,  
3150 Hz – 2.75 s, 4000 Hz – 2.15 s, 5000 Hz – 1.66 s.

In order to find out how the acoustic properties of the investigated screens are changing under the influence of weathering environment, the measurements of sound absorption were carried out at the initial stage and at time intervals after the successive aging tests. For that purpose, after every 50, 100 or 150 cycles, depending on the length of the test, the screens were dismantled from the aging chamber and moved over to the reverberation chamber to measure the sound absorption coefficient  $\alpha_s$  for 1/3 octave bands of the frequency from 100 to 5000 Hz, and then basing on the obtained results the sound absorption coefficient  $\alpha_w$  was determined as well as the sound absorption assessment  $DL_\alpha$  index. The particular samples of the panels were arranged in the horizontal position in the reverberation chamber (Fig. 4). The studies were carried out with the use of the measurement apparatus whose constituent parts meet the metrological requirements in terms of respective accuracy class for such

apparatuses. The screen samples were installed on the floor of the reverberation room having the volume of 202 m<sup>3</sup> one day before the test, in accordance with the method A (ISO 354, 2003). The reverberation times were determined by the interrupted noise method with 6 decay measurements made at each of the 6 microphone positions for each of the 2 loudspeaker positions to obtain a good average value at each of the one-third octave intervals in the range of 100–5000 Hz (ISO 354, 2003):

- 1) The transmission part of the test system consisted of the following elements: a column loudspeaker of spherical radiation characteristic, a generator of pink and white noise together with an amplifier.
- 2) The reception part of the test system comprised the following elements: a four-channel sound level gauge SVAN 958, two 1/2" microphones type SV22, two 1/2" microphone preamplifiers type SV22, an acoustic calibrator type SV03A, a PC computer with the software SvanPC+Software Official 1.0.21e. The tools had valid calibration certificates.
- 3) The panels were arranged together, obtaining the combined area of 12 m<sup>2</sup>, i.e. above 10 m<sup>2</sup> according to the standard recommendations (ISO 354, 2003) (Fig. 4). The measurements were carried out with stabilized thermal and humidity conditions at the temperature of  $+20\pm 2^\circ\text{C}$  and relative humidity of  $70\pm 5\%$ .

#### 2.4. SEM analyses

For the observation of morphology, the scanning electron microscope analysis (SEM) was carried out on the electron microscope TM 3000 Hitachi in the reflected electron flux augmented from 25 to 3000 times. The analysis was performed on a fracture surface at three stages: before the aging test, after 450 cycles and after 1000 cycles in order to observe if any changes were taking place on the panel components during the weathering process, and in particular on the surface of fiberglass and mineral wool fibers.

### 3. Results and discussion

#### 3.1. Results of acoustic measurements

For the assessment of acoustic quality, a single-number sound absorption evaluation index (ISO 1793, 2012) was accepted. The coefficient presents the values for octave bands (1) and corresponds to the values of sound absorption coefficient  $\alpha_S$  measured for 1/3 octave bands, in line with standard regulations (ISO 1793-1, 2012). The change of the values of the coefficient  $\alpha_S$ , dependent on frequency, into one number is in line with standard regulations (ISO 11654, 1997). When we know the values for  $DL_\alpha$ , we can classify the

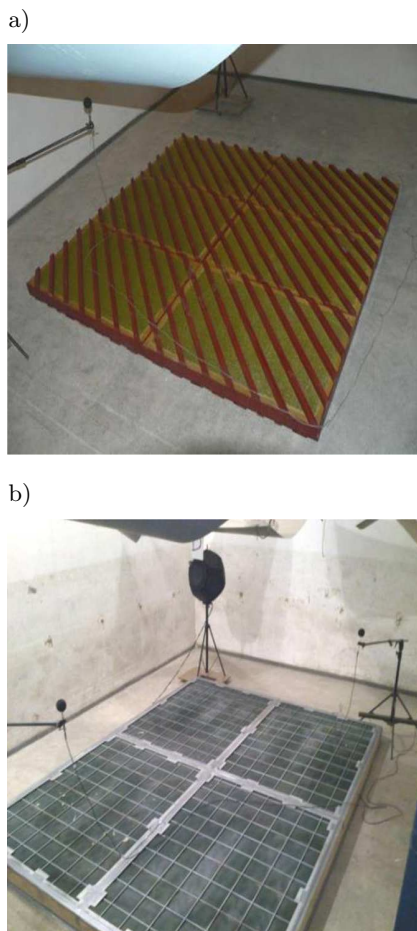


Fig. 4. Acoustic panels in the reverberation chamber: a) samples of timber panels type T1, b) samples of steel panels type S2.

acoustic screen in terms of absorbing properties, assigning an appropriate class in congruence with standard recommendations (ISO 1793-1, 2012). Basing on the above, for the investigated screens after successive aging stages, we determined the characteristics of sound absorption within the frequency of 100–5000 Hz (Figs. 5 and 6), the weighted sound absorption coefficient  $\alpha_w$  (ISO 11654, 1997) and the single-number sound absorption assessment index  $DL_\alpha$  (ISO 1793-1, 2012). For that purpose, after each 50, 100 or 150 cycles, depending on the duration of the test, the panels were dismantled from the aging chamber and moved over to the reverberation chamber where the measurements were carried out. The final values of the indexes are presented in Fig. 8

$$DL_\alpha = -10 \log \left| 1 - \frac{\sum_{i=1}^{18} \alpha_{si} 10^{0.1L_i}}{\sum_{i=1}^{18} 10^{0.1L_i}} \right|, \text{ dB} \quad (1)$$

where  $L_i$  is normalized sound level A, in dB, of roadside noise in the  $i$ -th third octave frequency band,  $\alpha_{si}$  is sound absorption coefficient in the  $i$ -th third octave frequency band.

We can observe an unexpected effect on the graphs in Fig. 5 where for the middle frequencies, the value of sound absorption coefficient  $\alpha_{si}$  higher than 1 was

obtained, whereas in terms of the standards the said value is contained within the interval  $\langle 0; 1 \rangle$ . Such a situation is quite common for the measurements in the reverberation chamber. As written by EVEREST (2001), scattering of sound at the edges of the research sample brings about the situation where such a sample in terms of acoustics seems to have a larger area than it has in reality, which leads to the acquisition if the sound absorption coefficient higher than 1. There is no standard method to make corrections in this respect.

The statistical analysis of the results was reduced to the correlation analysis. The objective of the analysis was to demonstrate that the sound absorption coefficient in the function of frequency had a similar run after each aging cycle. The aim of the analysis was not confined to the determination of acoustic parameters of a specific mineral wool of a given density, but it was supposed to demonstrate that the change of acoustic parameters could be affected by the aging process. In view of the above, the same panels of one of the acoustic screens were being subjected to the aging process in simulated conditions and to acoustic measurements.

When analysing the absorption results for the T1 panels (Fig. 5), we can observe that the runs of absorption coefficients  $\alpha_s$  as a frequency function before the aging test and after 100 and 150 cycles are very similar. In order to confirm the thesis stating that the changes of absorption coefficients  $\alpha_s$  as a frequency

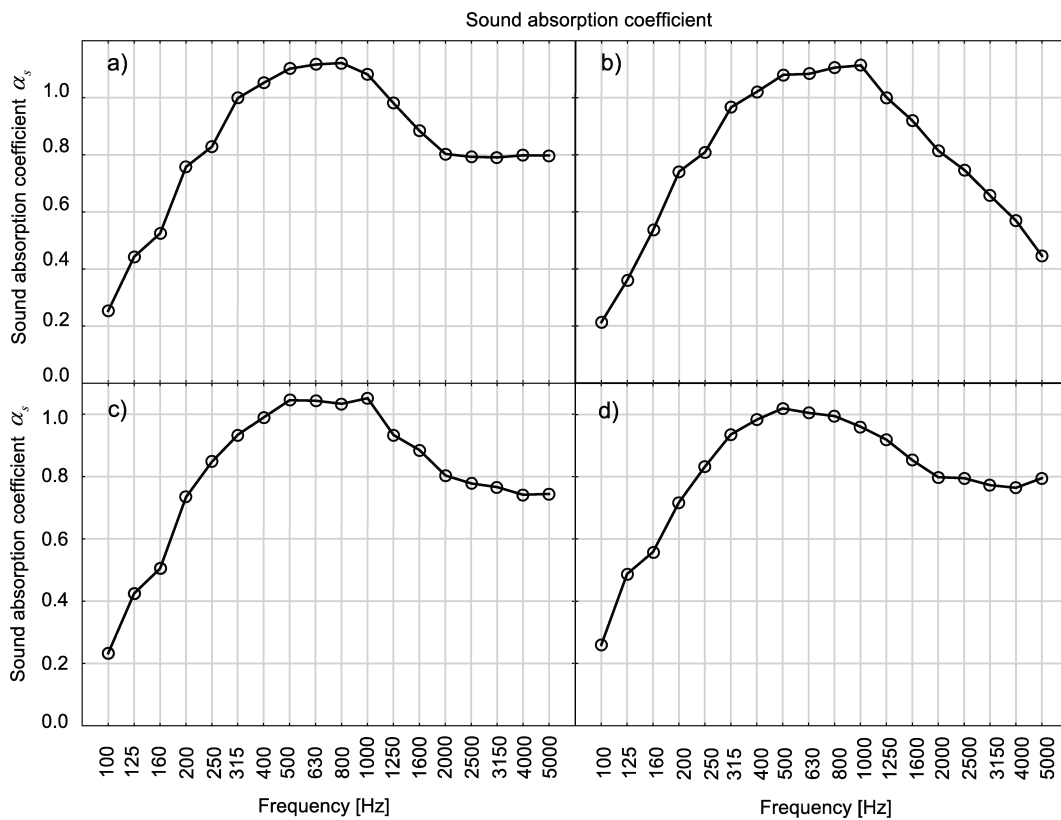


Fig. 5. Exemplary sound absorption characteristics for the panels of type T1: a) before the test, b) after 50 cycles, c) after 100 cycles, d) after 150 cycles of aging in the weathering chamber.

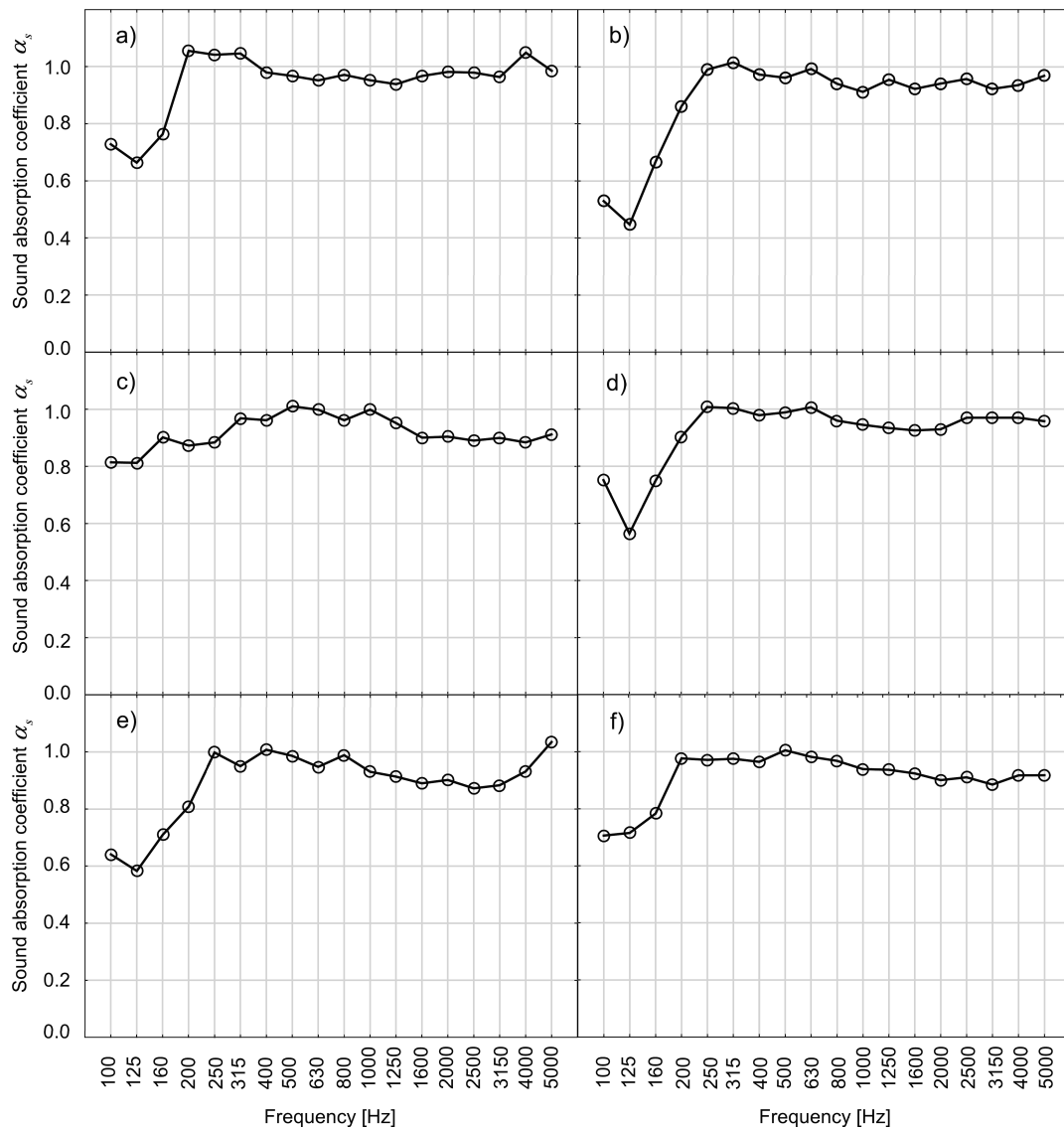


Fig. 6. Exemplary sound absorption characteristics for panels S2: a) before the test, b) after 100 cycles, c) after 238 cycles, d) after 300 cycles, e) after 400 cycles, f) after 500 aging cycles in the weathering chamber.

function before the test and after the test do not differ considerably, correlations were determined between the results before the test and after 50, 100 and 150 aging cycles respectively. It turned out that the correlation between the results before the test and after successive aging stages was as presented in Table 1.

Table 1. Correlations of absorption coefficients  $\alpha_s$  for the T1 panels before and after the tests.

Results of $\alpha_s$ before and after the tests	Correlation, $r$
50 cycles	0.93
100 cycles	0.99
150 cycles	0.99

All the obtained correlation coefficients were reached with the test probability  $p \ll 0.05$ , which be-

speaks of the fact that the results were statistically significant.

It was demonstrated that the characteristics  $\alpha_s$  in the frequency function are similar, and the numerical values of absorption coefficients differ depending on the aging time of the acoustic panels. Similar analyses can be done for the panes of type S2 whereof results are presented in Fig. 6.

We can see on the graphs in Fig. 6 that for the frequencies equal to and higher than 1000 Hz, the obtained sound absorption coefficients are within 0.8–1.0. Such a result is obtained through the application of a suitable mineral wool having very good acoustic parameters. These results are comparable to the results obtained by PLEBAN (2013).

When analysing the absorption results for the S2 panels (Fig. 6), we can observe that the runs of ab-

sorption coefficients  $\alpha_s$  as a frequency function before the aging test and after 100, 238, 300, 400 and 500 cycles are very similar. In order to confirm the thesis stating that the runs of absorption coefficients  $\alpha_s$  as a frequency function before the test and after the test do not differ considerably, correlations were determined between those results. It turned out that the correlation between the results before the test and after successive aging stages was as in Table 2.

Table 2. Correlations of absorption coefficients  $\alpha_s$  for the S2 panels before and after the tests.

Results of $\alpha_s$ before and after the tests	Correlation, $r$
100 cycles	0.92
238 cycles	0.47
300 cycles	0.91
400 cycles	0.84
500 cycles	0.90

All the obtained correlation coefficients were reached with the test probability  $p \ll 0.05$ , which bespeaks of the fact that the results were statistically significant. The only anomaly yielding the results which stood out was the correlation of the results before the test and after 238 cycles. We can also ob-

serve that for timber screens the runs were better correlated. However, the values of acoustic performance were lower. The panels of type S3 were analysed in the work (NOWOŚWIAT *et al.*, 2016) (Fig. 7), and therefore we have analysed here only the similarity between the runs of the sound absorption coefficient  $\alpha_s$  as a frequency function.

The correlation between the results before the test and after the successive aging stages is as presented in Table 3.

Table 3. Correlations of absorption coefficients  $\alpha_s$  for the S3 panels before and after the tests.

Results of $\alpha_s$ before and after the tests	Correlation, $r$
100 cycles	0.94
200 cycles	0.93
300 cycles	0.97
400 cycles	0.98
450 cycles	0.98
550 cycles	0.98
650 cycles	0.98
750 cycles	0.96
850 cycles	0.99
1000 cycles	0.96

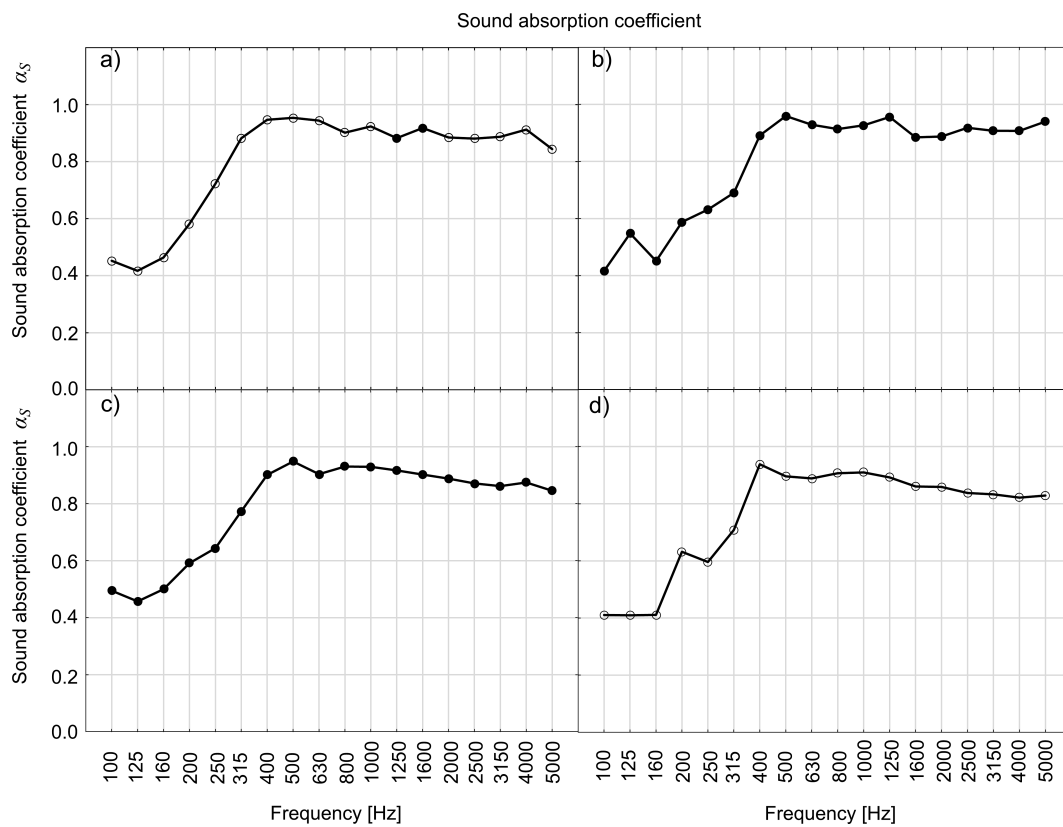


Fig. 7. Exemplary sound absorption characteristics for panels S3: a) at the initial stage, b) after 200 cycles, c) after 450 cycles, d) after 1000 cycles (NOWOŚWIAT *et al.*, 2016).



Basing on the determined characteristics  $\alpha_s$ , we determined the characteristics  $\alpha_w$  and  $DL_\alpha$ , which are presented in Fig. 8.

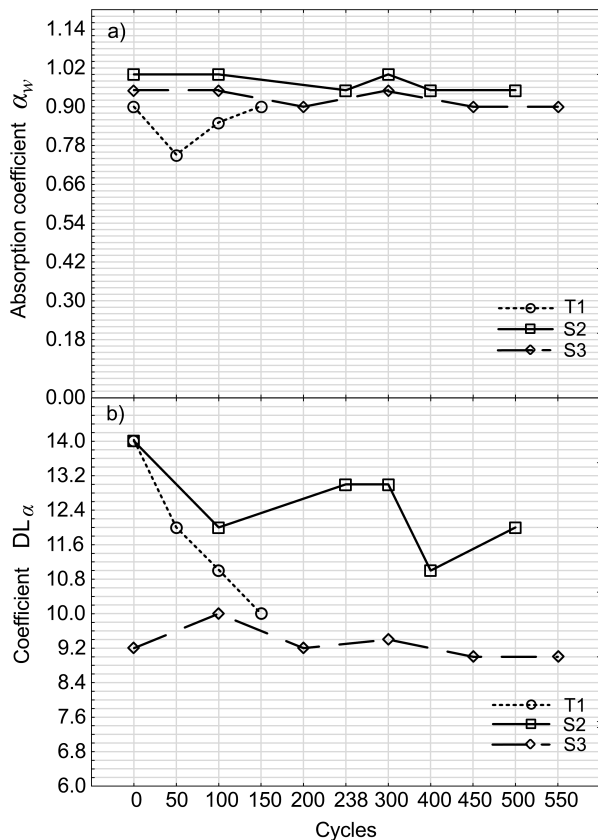


Fig. 8. a) Values of the weighted sound absorption coefficients  $\alpha_w$ , b) values of the single number sound absorption assessment indexes  $DL_\alpha$ .

For the particular values of the indexes  $\alpha_w$  and  $DL_\alpha$ , the measurement uncertainty was presented as the product of standard uncertainty and the coverage factor  $k_\alpha$ . The uncertainty was determined for the confidence level of  $p_\alpha = 95\%$  in accordance with the following algorithm (2), (3):

$$\delta_{95}(\alpha) = \frac{1.96 \cdot \varepsilon(\alpha)}{\sqrt{n}}, \quad (2)$$

where  $n$  is the number of measurements and  $\varepsilon$  stands for the combined uncertainty

$$\varepsilon(\alpha) \cong \frac{55.3V}{cS} \sqrt{\left(\frac{\varepsilon(T_2)}{T_2^2}\right)^2 + \left(\frac{\varepsilon(T_1)}{T_1^2}\right)^2}, \quad (3)$$

where  $\varepsilon(T)$  is the relative standard deviation (ISO 354, 2003),  $T_1$  is reverberation time of the empty room,  $T_2$  – reverberation time of the reverberation room after with the test specimen,  $V$  – volume of the reverberation room,  $c$  – the propagation speed of sound in air,  $S$  – the area, in square metres, covered by the test specimen.

Total measurement uncertainties are presented in Table 4.

Table 4. Ranges of measurement uncertainties.

	T1	S2	S3
$\delta_{95}(\alpha)$	0.005–0.07	0.001–0.02	0.19–0.21
$\varepsilon(DL_\alpha)$	0.65–0.74	1.45–1.69	0.59–0.66

The results obtained from the particular stages point out to the influence of the simulated aging. At the same time, we can observe that the results are different and depend on the design of the absorbing panels. The best sound absorption at the initial stage was demonstrated by timber panels and by slightly smaller panels of metal frame S2, which are characterized by a large number of layers, 6 layers (type T1) and 12 layers (type S2) respectively. The panels of the type S3, having a simplified system of five layers, did not actually demonstrate any changes. But the kinetics of changes in the particular panels turned out to be different. For timber panels after 150 aging cycles the value of index  $DL_\alpha$  decreased by 28%, whereas for the metal frame panels S2 after 500 cycles the absorption of sound decreased by 14%, and for the panels S3 after 450 cycles there were no changes. It may have been caused by a different way of covering the damping mat on the display side. In the panels T1 and S2, these layers are easily permeable for the pressure exerted by air or water, for example grid or fibrous layer. And in the panels S3, tight glass fabric was applied. This different structure of screens shows a different reaction to the impact of the external environment, and in particular rainwater. In the aging tests, we allowed for rainfall and impurities generated by vehicle exhaust fumes or de-icing salts. To simulate the impurities, we applied hard tap water. The calcium or magnesium ions present in such water, in the reaction with carbon dioxide present in the air, generate calcium carbonate which is deposited as sediment in the same way as sediments from impurities. The buildup of such light gray sediments was found via macroscopic tests during the aging tests on screen components from the display side.

### 3.2. Results of SEM observation

In order to find out whether the sediments imitating impurities have any impact on the main absorbing components, i.e. mineral wool mats, microscope observations of the surface morphology were carried out using the scanning method. In the particular tested screens, the observations involved all external components of the panels such as the grid (Figs. 9a,b), glass fabric (Figs. 9c,d) and surface layers of the mineral wool mats, 1–2 mm deep into the material (Figs. 9e,f). For the reference, the samples were collected from the

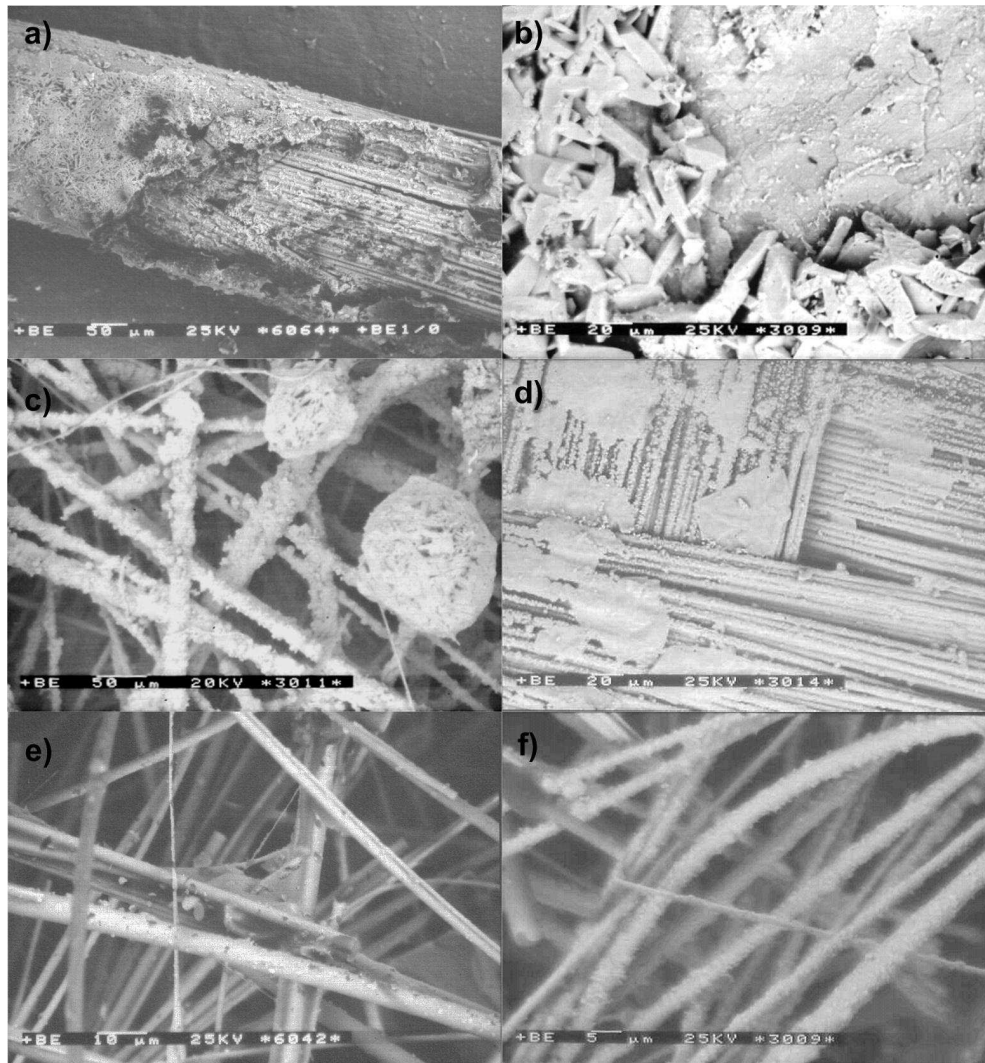


Fig. 9. Results of scanning observations: a) deposits of carbonates on the fiberglass grid in the screen type T1 after 150 cycles,  $\times 350$ , b) gypsum deposits on the fiberglass grid in the screen type S2 after 500 cycles,  $\times 1000$ , c) surface of glass fabric in the screen S2 after 500 cycles, thick deposits of carbonates,  $\times 500$ , d) deposits of calcium carbonates on fibrous glass in the screen S3 after 100 cycles,  $\times 800$ , e) deposits of carbonates on mineral wool fibers in the screen type T1 ( $\times 2500$ ) – after 150 cycles, f) fibers of mineral wool covered with carbonate deposit in the screen S3 after 450 cycles.

central and bottom parts of the screens. The images were made with the magnification from 100 to 3000 times.

Already after 100 cycles, we could observe on the surfaces of external materials deposits in the form of calcium carbonates  $\text{CaCO}_3$  precipitated from water (Fig. 9d), which corresponds with the changes of sound absorption of the screens, and in particular with respect to the standard solutions T1 and S2. In some places we could observe clusters of well developed, wide bars and clusters of cleavable crystals of square shape, probably gypsum  $\text{CaSO}_4 \cdot 2\text{H}_2\text{O}$  (Fig. 9b). In the successive stages of the aging tests, the amount of the deposits was increasing (Figs. 9a,c,f). Also in the contact places with glass fabric in the panels S2 we could observe a larger amount of deposits, which

means that the joints were not tight enough. Nevertheless, the structure of mineral wool fibers did not undergo any physical changes. The impact of aging was only manifested as the deposits of calcium carbonate precipitated from water to the depth of 1–2 mm (Figs. 9e,f). But in the S2 screen after 500 cycles, the fibers of mineral wool were slightly covered with the deposit (Fig. 9e) due to three-layered shield from grids and fibrous glass, which in turn had a heavy layer of deposits (Fig. 9c). A similar effect was found in the S1 screens. With such a solution the index  $\text{DL}_\alpha$  was reaching considerable values within the range of 10–14 dB (Fig. 8b). And in the timber screens T1, which also had three-layered shielding of wool mats, a considerable drop of the index  $\text{DL}_\alpha$  was observed, from 14 dB to 10 dB within a shorter test time of 150 cycles.

But in the screens S2, which had only one protective layer, the absorption turned out to be lower but more stable, within the range of 9–10 dB (Fig. 8b). In the bottom part of the screens less deposits could be observed than in the upper parts. Mineral wool mats are the main components absorbing sound in the screens. Therefore, the formation of deposits on mineral wool fibers and on the shielding grid or fabric (Fig. 9) can be the reason of the initial changes of the acoustic indexes  $DL_\alpha$  and  $\alpha_w$ . Hence, due to the impact of environmental factors, the acoustic class of screens can undergo changes.

#### 4. Prediction of acoustic durability

The characteristics of the index  $DL_\alpha$  (Fig. 8b) obtained from the research studies demonstrate decreasing trends. According to the standard classification (Table 5), acoustic screens can be ascribed acoustic classes depending on the obtained values of the index  $DL_\alpha$ . On that basis we can estimate the predicted changes of acoustic class of the screens during their service life in the atmospheric environment.

Table 5. Classes of absorption properties (ISO 11654, 1997).

Class	$DL_\alpha$ [dB]
A0	not defined
A1	< 4
A2	4–7
A3	8–11
A4	12–15
A5	> 15

Since durability is understood as the ability to satisfy certain definite serviceability requirements within a preset time period in some specific conditions. The analogous definition of “acoustic durability” is introduced in (EN 14389-1, 2015), defining the time period within which the deterioration of the acoustic parameters of the material will take place. The prediction of durability consists in satisfying the limit state of a particular serviceability characteristic. For that purpose, we need to define a measurable physical characteristic and its changes in the function of time  $C(t)$  and an arbitrary limit value  $C_{\min}$  defining serviceability requirements (BS ISO 15686-2, 2001). For the investigated screens, the measurable characteristic reflecting the aging process can be expressed by the changes of sound absorption of the screens, which is defined by the index  $DL_\alpha$ . The limit values can be accepted as particular classes of absorption properties (Table 5). In order to estimate the acoustic durability, for the measurement values of the index  $DL_\alpha$ , a trend analysis was carried out. The changes of acoustic characteristics of the screen after the successive aging cycles can be

treated as a time series. Trend in that case was treated as a systematic change of the value level of that series effected by certain permanent changes. Hence, to create a model curve, the method of time series seems to be an appropriate tool, which at the same time allows for random character of the problem through the statistical analysis. Such an approach is in line with the guidelines for the prediction of durability on the basis of accelerated aging tests (ASTM-G172-03). In order to analyse the trend, the simplest trend model was applied, that is a linear function in which the variable  $Y_t$  is linearly dependent on time  $t$ . In that case, when on the time series graph (Fig. 8b), an average decrease of the index  $DL_\alpha$  was reported by more or less the same value, a linear model of the trend function was proposed. The equation of the function is as follows:

$$y_t = \beta_0 + \beta_1 t + \xi_t, \quad (4)$$

where  $y_t$  is value of the variable  $Y$  for the time  $t$ ,  $\beta_0$ ,  $\beta_1$  stand for the parameters of the model,  $t$  – time,  $\xi_t$  – is the random variable defining the random element in the equation.

However, we must remember here that the random element should have zero expected value of the random elements and the variance of the random elements at each moment the same and equal to  $\sigma^2$ , and that the random vector  $\xi$  has the  $n$ -dimensional normal distribution.

In other words, the random elements must not have any tendency and should be so called white Gaussian noise. The appropriate fitting of the trend line with the data was obtained with the use of the least square method which, after the estimation of structural parameters assessment, yields the following equation:

$$\hat{y} = b_1 x + b_0. \quad (5)$$

Hence, the following was obtained for the type T1 screen:

$$y = -0.996x + 15.400. \quad (6)$$

Figure 9 presents the graph of the observed and predicted values with the use of Eq. (6).

As we can observe from Fig. 10, the description of the observed values with the Eq. (6) explains 99% of the results. The error of this estimation is 0.21. The test probability for the estimated gradient of the line is  $p = 0.004$ , and for the free term  $p = 0.003$ , which bespeaks of the statistical significance of the estimation. We also checked normal distribution of residuals and we obtained the test probability  $p = 0.97$  for the Shapiro-Wilk statistical test being 0.99291. Therefore, we can accept that on the significance level of  $\alpha = 0.05$  there are no grounds to reject the hypothesis stating normal distribution of residuals.

For the S2 screen, the linear trend does not reflect the character of the changes of  $DL_\alpha$  in the function

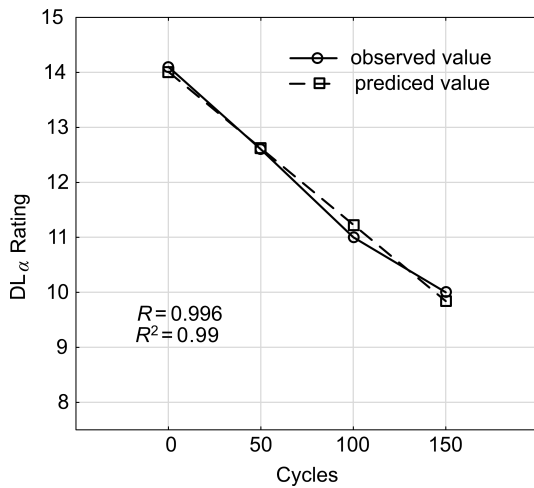


Fig. 10. Observed and predicted values.

of time. We did not also find any other polynomial which would reflect such a character of changes. In such a case, very frequently the methods of exponential smoothing or ARIMA are applied. But in our case we have too few measurement points (which are still very time-consuming to determine) to apply them. The said difficulties do not significantly hamper the conclusion making process involving the changes of acoustic parameters of the screen subjected to aging. Figure 11 presents the changes of the index  $DL_{\alpha}$  in the function of time together with the marked decreasing trend.

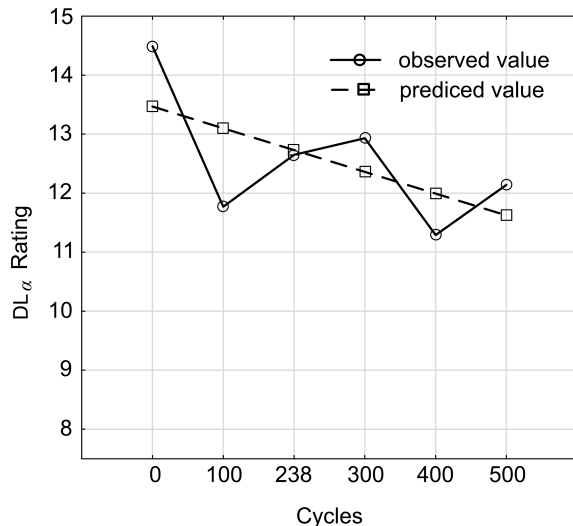


Fig. 11. Observed values and trend as a function of time.

The equation of the trend line has the form

$$y = -0.616x + 13.836. \quad (7)$$

As we can observe in Fig. 11,  $DL_{\alpha}$  has a decreasing trend with aging, as demonstrated by the line (7). For the S3 screen, the results were presented in the work (NOWOŚWIAT *et al.*, 2016), and here we only repeated

the equation of trend line verified statistically in the said work

$$y = -0.072x + 9.732. \quad (8)$$

The presented analysis makes it possible to predict the time after which the initial classes of absorption properties of the screens will reach the bottom limit. However, we allowed here for the level of weathering similarity that 100 cycles correspond with the time period of 2 years in the natural conditions of the Upper Silesian climate in Poland (ŚLUSAREK *et al.*, 2015). For the T1 screen, the value of  $DL_{\alpha}$  can be considerably changing after 150 cycles from 14 dB to 10 dB, and the equation describing it is correlated with the measurement values on a very high level of 0.996. We can therefore estimate that the value of the index  $DL_{\alpha}$  can reach the upper limit of class A3 after about 222 cycles, which in terms of natural conditions corresponds with the time period of 4.5 years. For the screen type S2, the value  $DL_{\alpha}$  of 11.0 dB will be reached after about 560 cycles, which corresponds with 11 years. And for the screen type S3 the value  $DL_{\alpha}$  of 8.0 dB will be obtained after 1150 cycles with the probability of 86%, staying within the interval (7.54, 8.47). Therefore, the value of the index  $DL_{\alpha}$  can reach the bottom limit of class A3 and change into class A2 after about 1150 cycles, which corresponds with the time period of 23 years in natural conditions.

## 5. Conclusions

The carried out investigation studies involving the acoustic properties of three road noise screen panels of different design subjected to simulated weathering have yielded the following conclusions:

- 1) The gathered results from the particular stages of simulated aging point out to the impact of weathering factors. The acoustic properties of sound absorption are not constant and have a decreasing tendency. It may be effected by the deposits on the components of the absorbing elements generated by urban pollution and communication impurities, including de-icing salts which in the aging tests had been simulated by the deposits of calcium carbonate precipitated from water which imitated rainfall, which was confirmed by the scanning analysis. Therefore, the acoustic properties of the screens during their service life can be changing, and the acoustic class defined at the initial stage can be decreasing.
- 2) The absorption of sound is considerably dependent on the design of panels and in particular on the system of layers and their permeability for water. The initial value of  $DL_{\alpha}$  index depends on the type and thickness of layers in the panel. In terms of the kinetics of changes, more advantageous absorption properties are exhibited by the

panels having tight fabrics from glass fibers. In the timber panels which do not have such a layer, the drop of  $DL_\alpha$  index after 150 cycles turned out to be higher and reached 21.5%. For the panels of metal design with a tighter layer, the drop of the  $DL_\alpha$  index after 500 cycles was not higher than 8.4%. And the panels with tight glass fabric after 450 cycles did not demonstrate any change involving the class of absorbing properties.

- 3) The changes of sound absorption combined with the weathering similarity of the aging chamber (100 cycles = 2 years) allow us to predict the acoustic service life of the panels with respect to the standards of acoustics classes. It is useful to apply for that purpose the analysis of  $DL_\alpha$  index, using the method of time series, which apart from the modeling capabilities allows also for the random character of the problem. It makes it possible to verify acoustic classes and to estimate their changes in service life. For the investigated screens of the type T1 and S2, basing on the measured kinetics of acoustic absorption changes, we can state that the classes can undergo changes respectively: to the class A3 over the time period of 3 years and to the class A4 over 10 years. And for the screens S3, the acoustic absorption will not change over 9 years.

### Acknowledgments

The realization of the research studies was possible thanks to the cooperation and financial support of the companies: Gomibud from Poland and Rockwool B.V. from Holland and also thanks to technical supervision of the aging chamber offered by the company Clanet from Gliwice.

### References

1. ASTM-G172-03 (2010), *Standard guide for statistical analysis of accelerated service life data*.
2. BASIŃSKA M., KOCZYK H. (1995), *External climate in study and models* [in Polish], 3rd Scientific-Technical Conference "Building Physics in Theory and Practice", pp. 14–21.
3. BOCHEN J. (2010–2013), *Durability prediction of building components exposed to natural weathering on the ground of accelerated ageing tests*, Research Project PBU-33/RB9/2010.
4. BROLIN H. (1984), *Dimensional stability of entrance doors exposed to natural climate*, 3rd International Conference on the Durability of Building Materials and Components, VTT Symposium, Espoo, **2**, 12–20.
5. BS EN 14389-1: 2015 (2015), *Road traffic noise reducing devices. Procedures for assessing long term performance. Acoustical characteristics*.
6. BS ISO 15686-2: 2001 (2001), *Buildings and constructed assets – Service life planning. Part 2: Service life prediction procedures*.
7. BUTTERVORTH B. (1964), *The recording comparison and use of outdoor exposure tests*, Transactions of the British Ceramic Society, **63**, 11, 105–116.
8. CASTIÑEIRA-IBÁÑEZ S., SÁNCHEZ-PÉREZ J.V. (2015), *Environmental noise control during its transmission phase to protect buildings. Design model for acoustic barriers based on arrays of isolated scatterers*, Building and Environment, **93**, 2, 179–185.
9. DELANEY M.E., BAZLEY E.N. (1970), *Acoustic properties of fibrous absorbent materials*, Applied Acoustics, **3**, 2, 105–116.
10. DING S.H., LIU D.Z. (2006), *Durability evaluation of building sealants by accelerated weathering and thermal analysis*, Construction and Building Materials, **20**, 10, 878–881.
11. EVEREST F.A. (2001), *Master handbook of acoustics*, McGraw Hill, USA.
12. FUJIWARA K., ANDO Y., MEAKAWA Z. (1977), *Noise control by barriers. Part 1: noise reduction by a thick barrier*, Applied Acoustics, **10**, 2, 147–159.
13. FUJIWARA K., ANDO Y., MEAKAWA Z. (1977), *Noise control by barriers. Part 2: noise reduction by a thick barrier*, Applied Acoustics, **10**, 3, 167–179.
14. FUJIWARA K., HOTHERSALL D.C., KIM C. (1998), *Noise barriers with reactive surfaces*, Applied Acoustics, **53**, 4, 255–272.
15. GARAI M., GUIDORZI P. (2000), *European methodology for testing the airborne sound insulation characteristics of noise barriers in situ: Experimental verification and comparison with laboratory data*, Journal of the Acoustical Society of America, **108**, 3, 1054–1067.
16. GARAI M., GUIDORZI P. (2008), *In situ measurements of the intrinsic characteristics of the acoustic barriers installed along a new high speed railway line*, Noise Control Engineering Journal, **56**, 5, 342–355.
17. GUIDORZI P., GARAI M. (2013), *Advancements in sound reflection and airborne sound insulation measurement on noise barriers*, Open Journal of Acoustics, **3**, 2A, 25–38.
18. HADDEN J.W., PIERCE A.D., KIM C. (1981), *Sound diffraction around screens and wedges for arbitrary point source location*, Journal of the Acoustical Society of America, **69**, 4, 1060–1064.
19. ISHIZUKA T., FUJIWARA K. (2004), *Performance of noise barriers with various edge shapes and acoustical conditions*, Applied Acoustics, **65**, 2, 125–141.
20. ISO 11654: 1997 (1997), *Acoustics – Sound absorbers for use in buildings – Rating of sound absorption*.
21. ISO 354: 2003 (2003), *Acoustics – Measurement of sound absorption in a reverberation room*.

22. ISO 1793-1: 2012 (2012), *Road traffic noise reducing devices. Test method for determining the acoustic performance. Intrinsic characteristics of sound absorption*.
23. JOANSSON H.G. (1972), *Diffraction by wedges of finite acoustic impedance with application to depressed roads*, Journal of Sound and Vibration, **25**, 4, 577–585.
24. KAMISIŃSKI T., KINASZ R., SZELĄG A., RUBACHA J., PILCH A., FLACH A., BARUCH K. (2015), *The comprehensive research of the road acoustic screen with absorbing and diffusing surface*, Archives of Acoustics, **40**, 1, 137–144.
25. KRAS P., OWERKO T., ORTYL Ł., KOCIERZE R., SUKTA O., PRADELOK S. (2012), *Advantages of radar interferometry for assessment of dynamic deformation of bridge. Bridge maintenance, safety, management, resilience and sustainability*, Proceedings of the 6th International IABMAS Conference, Stresa Lake Maggiore, Italy, 8–12 July 2012, pp. 885–891.
26. KURZE U.J., ANDERSON G.S. (1971), *Sound attenuation by barriers*, Applied Acoustics, **4**, 35–53.
27. KUS H., CARLSSON T. (2003), *Microstructural investigations of naturally and artificially weathered autoclaved aerated concrete*, Cement and Concrete Research, **33**, 9, 1423–1432.
28. LANAS J., SIRERA R., ALVAREZ J.I. (2006), *Study of the mechanical behavior of masonry repair lime-based mortars cured and exposed under different conditions*, Cement and Concrete Research, **36**, 5, 961–970.
29. LI K.M., WONG H.Y. (2005), *A review of commonly used analytical and empirical formulae for predicting sound diffracted by a thin screen*, Applied Acoustics, **66**, 45–76.
30. LITHERLAND K., OAKLEY D., PROCTOR B. (1981), *The use of accelerated ageing procedures to predict the long term strength of GRC composites*, Cement and Concrete Research, **11**, 3, 455–466.
31. MARTINEZ-RAMIREZ S., PUERTAS F., BLANCO-VARELA M., THOMPSON G. (1997), *Studies on degradation of lime mortars in atmospheric simulation chambers*, Cement and Concrete Research, **27**, 5, 777–784.
32. MAY D.N., OSMAN N.M. (1980), *Highway noise barriers: new shapes*, Journal of Sound and Vibration, **71**, 1, 73–100.
33. MEAKAWA Z. (1968), *Noise reduction by screens*, Applied Acoustics, **1**, 3, 157–173.
34. MIN H., QIU Q. (2009), *Multiple acoustic diffraction around rigid parallel wide barriers*, Journal of the Acoustical Society of America, **126**, 1, 179–186.
35. MONAZZAM M.R., LAM Y.W. (2005), *Performance of profiled single noise barriers covered with quadratic residue diffusers*, Applied Acoustics, **66**, 709–730.
36. MORANDI F., MINIACI M., MARZANI A., BARBARESI L., GARAI M. (2016), *Standardised acoustic characterisation of sonic crystals noise barriers: Sound insulation and reflection properties*, Applied Acoustics, **114**, 294–306.
37. MOROPOULOU A., HARALAMPOULOS G., TSIOURVA T., AUGER F., BRIGINIE J.M. (2003), *Artificial weathering and non-destructive tests for the performance evaluation of consolidation materials applied on porous stones*, Materials and Structures, **36**, 4, 210–217.
38. MOTOHOSHI K., NIREKI T. (1984), *Investigation into degradation mechanisms for masonry coating systems by microscopic analysis methods*, 3rd International Conference on the Durability of Building Materials and Components, VTT Symposium, Espoo, **2**, 241–253.
39. MURATA K., NAGAKURA K., KITAGAWA T., TANAKA S. (2006), *Noise reduction effect of noise barrier for Shinkansen based on Y-shaped structure*, Quarterly Report of Railway Technical Research Institute of RTRI, **47**, 3, 162–168.
40. NOWOŚWIAT A., BOCHEN J., DULAK L., ŻUCHOWSKI R. (2016), *Investigation studies involving sound absorbing parameters of roadside screen panels subjected to aging in simulated conditions*, Applied Acoustics, **111**, 8–15.
41. PARNELL J., SAMUELS S., TSITSOS C. (2010), *The acoustic performance of novel noise barrier profiles measured at the roadside*, Acoustics Australia, **38**, 3, 123–128.
42. PAVLIK Z., JURICKOVA M., CERNY R. (2004), *Semi-scale testing of multi-layered building envelope on basis of HPC in difference climate conditions*, Annual of Civil Engineering, **4**, 17–24.
43. PIERCE D. (1974), *Diffraction of sound around corners and over wide barriers*, Journal of the Acoustical Society of America, **55**, 5, 941–955.
44. PIHLAJAVAARA S.E. (1984), *The prediction of service life with the aid of multiple testing, reference materials, experience data and value analysis*, 3rd International Conference on the Durability of Building Materials and Components, VTT Symposium, Espoo, **2**, 37–164.
45. PLEBAN D. (2013), *Method of Testing of Sound Absorption Properties of Materials Intended for Ultrasonic Noise Protection*, Archives of Acoustics, **38**, 2, 191–195.
46. RUDNO-RUDZIŃSKA B., MALEC T., SAWA Ł. (2008), *Influence of meteorological conditions on effectiveness of acoustic screens-measurements and computations*, Archives of Acoustics, **33**, Supplement, 71–76.
47. SAMUELS S., ANCIH E. (2001), *Recent developments in the design and performance of road traffic noise barriers*, Acoustics Australia, **29**, 2, 73–78.
48. ŚLUSAREK J., BOCHEN J., DULAK L., ŻUCHOWSKI R., NOWOŚWIAT A. (2014), *Research on sound absorption of noise barriers subjected to accelerated ageing test of 400 cycles*, Research U-776/RB-3/2013 for Rockwool B.V, the Netherlands.
49. ŚLUSAREK J., BOCHEN J., DULAK L., ŻUCHOWSKI R., NOWOŚWIAT A. (2015), *Research on sound absorption*

- of noise barriers subjected to accelerated ageing test of 550 cycles, Research U-717/RB-3/2014 for Rockwool B.V, the Netherlands.
50. UEMOTO K.L., FLAUZINO W.D. (1984), *Natural and accelerated ageing of GRP and PVC corrugated sheets*, 3rd International Conference on the Durability of Building Materials and Components VTT Symposium, Espoo, **2**, 135–146.
  51. WATTS G., MORGAN P.A. (1996), *Acoustic Performance of an Interference-Type Noise-Barrier Profile*, *Applied Acoustics*, **49**, 1, 1–16.
  52. WATTS G. (2000), *Factors affecting the performance of traffic noise barriers*, 29th International Congress and Exhibition on Noise Control Engineering, Inter Noise, Nice, France.
  53. YILMAZER S., OZDENIC M.B. (2005), *The effect of moisture content on sound absorption of expanded perlite plates*, *Building and Environment*, **40**, 3, 311–318.
  54. YIU C.Y., HO D.C., LO S.M. (2007), *Weathering effects on external wall tiling systems*, *Construction and Building Materials*, **21**, 3, 594–600.